DOI: 10.1021/ma901378t

Macromolecules
ARTICLE

Water-Soluble Cationic Aromatic Dendrimers and Their Complexation with DNA

Zinaida B. Shifrina,[†] Nina V. Kuchkina,[†] Pavel N. Rutkevich,[§] Tatyana N. Vlasik,[§] Anna D. Sushko,[‡] and Vladimir A. Izumrudov*,[‡]

[†]*A.N.Nesmeyanov Institute of Organoelement Compounds, Russian Academy of Sciences, Vavilov st., 28, Moscow, 119991 Russia,* [§]*Federal State Institution (FSI) Russian Cardiology Research-Industrial Complex, Russian Ministry of Health, 3 Cherepkovskaya st., 15a, Moscow, 121552 Russia, and* [‡]*M.V. Lomonosov Moscow State University, Chemistry Department, Leninsky Gory, Moscow, 119991 Russia*

Received June 26, 2009; Revised Manuscript Received November 7, 2009

ABSTRACT: Water-soluble cationic polypyridylphenylene dendrimers (wPPPDs) of different generations and various contents of pyridyl and phenylene moieties were synthesized. Interaction of wPPPDs with DNA resulted in the formation of polyelectrolyte complexes stable at physiological pH and ionic strength. Noticeable contribution of hydrophobic interactions provided by phenylene groups of the dendrimer in the complex stability was ascertained. Data obtained by turbidimetry and a sedimentation assay, as well as ζ-potential measurements, strongly implied the inaccessibility of positively charged pyridinium groups situated in the inner part of the dendrimer molecules for interaction with the rigid double helix. Positively and negatively charged water-soluble nonstoichiometric polyelectrolyte complexes were prepared and phase separations in their water-salt solutions were investigated. According to DLS measurements supported by the sedimentation assay, the addition of wPPPD in DNA solution in a wide range of the mixture composition (before phase separation) led to two coexisting populations of nanoparticles related to the soluble DNA/wPPPDs complex and practically unbound DNA. The revealed spontaneous formation of nanoparticles of the positively charged soluble DNA/wPPPDs complexes stable at ionic strength close to the physiological one is extremely encouraging for the development of the wPPPD vehicle to deliver gene materials to the cell.

Introduction

Since the pioneering works by Vogtle,[1] Tomalia,[2,3] and Newkome[4] an interest in dendrimers and hyperbranched polymers has been increased tremendously (e.g., see review articles[5−17]). Dendrimers are well-defined, highly branched macromolecules that radiate from a core and are synthesized through a stepwise repetitive reaction sequences. This guarantees complete shell for each generation, leading to monodisperse polymers. The synthetic procedures developed for dendrimers preparation allow control over molecular weight, topology, cavity size and surface modification.[6,13,18] The exceptional combination of structural perfection, high density and well-defined number of terminal groups that might be chemically different from interior ones, facilitate the development of functional nanoscale materials with unique electronic, optical, opto-electronic, magnetic, chemical, or biological properties. They could form the basis of new nanoscale materials and devices.[13,19−21]

The water solubility of representatives of some dendrimer families has been the focus of researchers that develop the problems of delivery the physiologically active compounds to target cell nuclei.[22−29] Thus, the use of the most extensively studied water-soluble polyamidoamine (PAMAM) or polypropylenimine (DAB-$(NH_2)_n$) dendrimers of different generations allows one to enhance considerably the transfection activity of plasmid DNA and oligonucleotides into cells. Such dendrimers are commercially available and commonly exploited for the targeting of the genetic material in vitro. Complexes of hard spheres (macroions) and oppositely charged linear polyelectrolyte have been studied extensively by theoretical modeling[30−40] and computer simulations.[41−46] The complexation in systems containing more than two macroions has been addressed by Nguyen and Shklovskii,[34,36,40] Kunze et al.[33] and Schiessel et al.[38] Wallin and Linse performed a series of Monte Carlo simulations including determination of the free energy of the formation of complexes between macroions and the polyion.[41−44] Computer simulations have recently been performed on dendrimers with charged terminal groups and oppositely charged linear chains by Welch and Muthukumar,[47] Lyulin et al.,[48,49] and Maiti et al.[50] In the most recent paper by Qamhieh et al. the theoretical model of the complex formation has been applied to study the structure of DNA/dendrimer complex. Model was based on experimental data for the formation of aggregates between DNA of different lengths and PAMAM dendrimers of generation 4.[51]

Despite a numerous publications on dendrimers as potential carriers for delivery of biological materials (e.g., see review article[23]), some key aspects of their interaction with structural parts of the biological cell remain unknown that presents problems in design of effective systems for targeted transport of gene material. For the development of dendrimer gene therapy, fundamental study of interaction of water-soluble cationic dendrimers with negatively charged components of the cell, specifically proteins (enzymes) and nucleic acids appears to be crucial. Remarkably, little is known of how complex formation, i.e., the size and the structure of the complexes, is governed by the chain stiffness and by the chain topology of the polycations utilized, except for some indirect evidence for dendrimers of various generations.[52−56] Published papers on such investigations[52,53,57−59] concern DNA complexation with different generations of dendrimers of one

*Author to whom correspondence should be addressed. E-mail: izumrud@genebee.msu.ru.

 Published on Web 11/24/2009

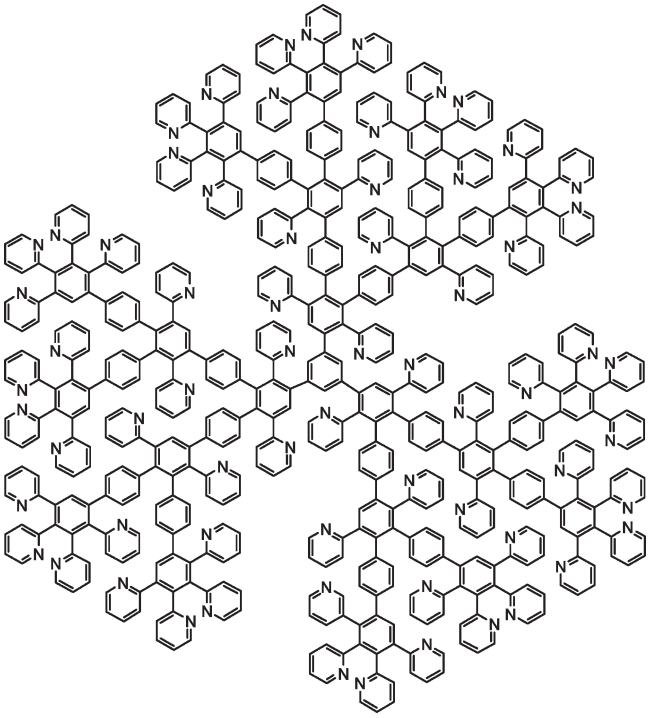

Figure 1. Third generation polypyridylphenylene dendrimer.

family. The dendrimers had one property in common, i.e., the same order in the arrangement of charged groups within the dendrimer molecule which was predetermined by the synthetic approach. The lack of possibility to vary both the topology of the functional groups and their relative content in the molecule of a given generation is a drawback that imposes the restriction on elaborating the criteria for preparation of effective dendrimer carriers.

Polypyridylphenylene dendrimers (PPPDs) that were synthesized by us recently[60] constitute the family of entirely aromatic dendrimers that might be promising model objects for above experiments. Figure 1 shows PPPD molecule of the third generation.

PPPDs offer several advantages over dendrimers synthesized to date. In contrast to extensively studied dendrimers containing flexible single bonds, the aromatic dendrimers are stiff as the rotation is only possible around the inter-ring C−C bonds. Such mobility does not noticeably affect the overall shape of the dendrimers, i.e. they are shape persistent nanoparticles.[61] This endows dendrimer molecule with 3D-structure that remains highly symmetric even in the case of high generations and also allows the control over functionality that can be positioned in predetermined sites of the molecule. As a consequence, one can suggest further potential control and tunability with respect to assembles formed by dendrimers with the partners of different nature, specifically different biological objects. Furthermore, the number of functional groups in PPPD molecules is specified by the conditions of synthesis and the arrangement of these groups can be varied deliberately from a uniform distribution to a pronounced accumulation at the periphery or in the core of the PPPD molecule.

There is an advantage that sets apart PPPDs from the other rigid aromatic dendrimers and is crucial for our case. Recently,[62] we have reported that alkylation of pyridyl groups in PPPDs yielding quaternized pyridinium cations resulted in formation of water-soluble dendrimers (wPPPDs). The use of water-soluble cationic analogues of PPPDs might provide important information on the influence of charge density, hydrophilic−lipophilic balance, and topology of the dendrimer functional groups on efficacy of the dendrimer interaction with nucleic acid. The data on the topology could be of particular interest. Thus, for polypropylenimine dendrimers, the ability to form water-soluble complexes with DNA has been assigned to poor availability of protonated amino groups situated in the inner part of the dendrimer for negatively charged phosphate groups of the rigid double helix.[57] This prevents complete neutralization of the charges and favors the soluble complex formation. In stiff wPPPD molecules that contain a large number of phenylene groups, the availability of the interior pyridinium cations for the electrostatic interaction could be particularly low and hence, the formation of the soluble complexes is facilitated. In the current work, this assumption is strongly supported by the experimental data that will be discussed below. Notice that the results obtained on studying the DNA/wPPPD system could be particularly promising for theoretical modeling. The point is that the reported theoretic model investigations are based on complexation of a polyelectrolyte with an oppositely charged spherical macroion which are mostly considered as hard sphere. Meanwhile, more realistic model has been proposed recently[51] for the available cationic dendrimers that should be regarded as soft spheres since their diameter is evidently decreased upon neutralization of the surface charges by the bound polyanion. Contrary to aliphatic flexible PAMAM or polypropylenimine dendrimers, aromatic rigid wPPPD molecules possess distinct 3D-structure that remains practically unchanged upon the complexing and hence, can be actually conceived as hard spheres. A comparison of the behavior of dendriplexes formed by the flexible and rigid dendrimers could be crucial for verification of the developed theoretical models.

Herein, we report the synthesis of different generations of wPPPDs with varied hydrophobicity and the investigation of the dendrimer interaction with native DNA. Particular emphasis has been placed on formation of water-soluble polyelectrolyte complexes and phase separations in their solutions, specifically caused by the added salt. It was found that even wPPPDs of younger generations form DNA−dendrimer complexes that are stable at physiological pH and ionic strength presumably due to noticeable contribution of hydrophobic interactions (provided by phenylene groups of the dendrimers) in the complex stability. Data obtained on studying the model systems can serve as foundation for the development of dual-purpose drugs in which the dendrimer vehicle combines the abilities to transfect genetic material to cell nuclei and deliver hydrophobic low-molecular-weight pharmaceutical agents to the cell.

Experimental Section

Materials. NaOH, HCl, 3-(4,5-dimethylthiazol-2-yl)-2,5-diphenyltetrazolium bromide (MTT), TRIS, and HEPES buffers were purchased from Sigma (St. Louis, MO). In all experiments, twice-distilled water purified by Milli-Q (Millipore, U.S.A.) was used. Dulbecco's modified Eagle's media (DMEM), fetal bovine serum, L-glutamine, penicillin, streptomycin, phosphate buffer saline (PBS) and lipofectamine 2000 reagent were purchased from Invitrogene, USA. Expression plasmid pC4W-KCopGFP driven by cytomegalovirus promoter was obtained from Mona Ltd., Russia. Ethidium bromide (EB) was purchased from Sigma and used as obtained. Concentration of EB in solution was determined spectrophotometrically assuming molar extinction coefficient 5600 L mol^{-1} cm^{-1} at 480 nm.[63] The sodium salt of highly polymerized calf thymus DNA (~10000 base pairs) was purchased from Sigma and used without purification. Concentration of DNA phosphate groups in the solutions was determined by absorbance at 260 nm assuming molar extinction coefficient ε_{260} = 6500 L mol^{-1} cm^{-1}.[64] Polypropyleneimine dendrimer DAB-NH_2-16 (Astramol) of the third generation bearing 16 primary amino

groups in the molecule was purchased from Aldrich and used as obtained. Poly(*N*-ethyl-4-vinylpyridinium) bromide (PEVP) was prepared by exhaustive alkylation of poly(4-vinylpyridine), DP 340 with ethyl bromide as described elsewhere.[65] Samples of polymethacrylic acid of different DP ranging from 1840 to 12 were purchased from Polysciences (U.S.A.). Sodium polystyrenesulfonates of different DP ranging from 1710 to 8 were commercial samples of Serva (Germany).

Characterization Techniques. ^{1}H NMR spectra were recorded with a Bruker AMX 600 MHz using D_2O as solvent. IR spectroscopy was performed using a ThermoNicolet AVATAR 370 FTIR spectrometer (Thermo Electron Corporation, Waltham, MA).

Dendrimer Synthesis. Parent PPPDs of the first, second, third, and forth generations as well as the PPPDs that contained reduced amount of pyridyl groups were synthesized, purified, and characterized as described elsewhere.[60] Water-soluble cationic dendrimers wPPPDs were prepared by alkylation of PPPDs pyridyl groups with dimethylsulfate in methanol according to Menshutkin reaction. The course of the alkylation was monitored by IR spectroscopy of the probes that indicated both a successive growth in absorbance of quaternized pyridinium moieties (ν = 1640 cM^{-1}) and reduction in absorbance of nonalkylated pyridyl moieties (ν = 1600 cM^{-1}).[66] The alkylation degree β, %, was determined from ^{1}H NMR spectra by the ratio of signals of the protons of methyl groups and aromatic fragments. Besides, the alkylation degree was calculated from the content of sulfur in the dendrimers samples which was ascertained by the elements analysis. Under experimental conditions (4 h, 25 °C, 10^{-3} mol· L^{-1} pyridyl groups, and 2×10^{-3} mol ·L^{-1} dimethyl sulfate) the values of β varied for different samples in the range of 87 ± 5%.

Spectrophotometry measurements were performed using a Hitachi 150−20 spectrometer (Japan) in a water-thermostatic cell at 25 °C.

Fluorescence Measurements. Fluorescence intensity I of the solutions was measured using a Jobin Yvon-3CS spectrofluorimeter (France) with water-thermostatic stirred cell holder. The measurements were made in a capped quartz fluorescence cell upon permanent stirring at 25 °C. The excitation and emission wavelengths in experiments with ethidium bromide were set at 535 and 595 nm, respectively. Concentrations of ethidium bromide and phosphate groups before titration were 1×10^{-5} M and 4×10^{-5} M, respectively; i.e., the ratio [EB]/[P] was 0.25.

Sedimentation Assay. Solutions of wPPPD and DNA prepared in 0.01 M HEPES buffer (pH = 7.2) were mixed at a given [+]/[−] ratio (where [+] and [−] are the molar concentrations of the pyridinium groups and phosphate groups, respectively) in the absence or presence of sodium chloride and centrifuged (11000 g, 10 min.). Concentration of pyridinium groups in the supernatants was determined by absorbance at 310 nm and normalized to the initial concentration of the groups that was 2×10^{-4} M in all mixtures. The experiments were conducted at 25 °C.

ζ-Potential measurements were performed using Zetasizer Nano-ZD (Malvern Instruments). Concentration of negatively charged groups of DNA or synthetic polyanions was 1.6×10^{-5} M before titration of their solutions with the dendrimer solution. Experiments were carried out in 0.01 M HEPES buffer (pH = 7.2) or TRIS buffer (pH = 9) at 25 °C.

Turbidimetric Titration. Mixtures of wPPPD and DNA solutions prepared in 0.01 M HEPES buffer (pH = 7.2) at a given [+]/[−] ratio was titrated with concentrated (4 mol·L^{-1}) solution of sodium chloride. Time interval between the salt adding was 2 min except the mixtures containing the dendrimer of the forth generation that were titrated with 5 min interval. The turbidity was estimated by absorbance at λ = 450 nm. Concentration of the dendrimer pyridinium groups in all mixtures was 2×10^{-4} M. Experiments were performed at 25 °C.

Dynamic Light Scattering. Measurements were conducted using ALV/DLS/SLS-5022F Compact Goniometer System from ALV-GmbH, Germany equipped with He−Ne laser (632.8 nm, 22 mV) at angles ranging from 30° to 150° (in 15° step) at 25 °C. The samples were prepared in 0.01 M HEPES buffer (pH 7.0) using twice-distilled water. Concentration of phosphate groups was [P] = 9×10^{-5} M. Data analysis was performed by inverse Laplace transformation under regularization with the use of CONTIN, and the calculated diffusion coefficients were extrapolated to zero scattering vector. The hydrodynamic diameter was determined from the Stokes−Einstein relationship.

AFM Imaging. AFM images were recorded on Solver P47−H (NT-MNT Russia) in tapping mode regime at room temperature. A silicon cantilevers fpN01 (NIIFP Russia) with 11.5 N m^{1-} typical spring constant and nominal tip radius < 10 nm were used. Typical working frequency was about 200 kHz. The topography data was processed by FemtoScan program (ATC, Russia) by flattering and lines adjusting.

Mica was used for DNA and dendrimer samples while the sample of the DNA/dendrimer mixture was deposited on highly ordered pyrolytic graphite (HOPG).

A 5 μL of pC4W-KCopGFP-linear DNA solution (C = 0.01 g L^{-1},) containing 1 mM $MgCl_2$ was deposited on freshly cleaved mica surface, incubated for 10 min, rinsed with Millipore Milli-Q deionized water for 1 h and air dried. A 5 μL of the dendrimer solution (C = 0.001 g L^{-1}) was deposited on freshly cleaved mica surface, incubated for 10 min, rinsed with Millipore Milli-Q deionized water for 1 min, and air drying.

Complex of DNA with wPPPD was prepared as follows. Solution of the components were dissolved in HEPES (0.01M) to the final concentration of C = 0.001 g L^{-1} Then the DNA solution was added dropwise under stirring into the dendrimer solution to reach the desired charge ratio and incubated at room temperature for 1 h. A 20 μL aliquot of the prepared sample was deposited on a surface of freshly cleaved HOPG, incubated for 10 min, rinsed with Milli-Q water, and air dried.

High-Speed Sedimentation Assay. Sedimentation velocity experiments were performed with a Beckman-E ultracentrifuge equipped with absorbance scanner device (Beckman Coulter, USA). An An50 Ti eight-hole rotor for 400-μL samples that were placed in standard double-sector Epon centerpieces with sapphire windows was used. DNA solution and solutions of DNA mixtures with wPPPD of different composition [+]/[−] were centrifuged (46000 rpm) under permanent scanning at 260 nm. Concentration of DNA phosphate groups in all experiments was the same and equaled to 1.0×10^{-4} mol·L^{-1}. The contribution in the absorbance of wPPPD was taken into account, and the corresponding corrections were made. Values of the coefficient of sedimentation were estimated from the sedimentation patterns using computer program SEDFIT which was developed in National Health Institute (USA). The program is free and available on the Internet (http://www.analyticalultracentrifugation.com/default.htm). The experiments were conducted at 25 °C.

In Vitro Cell Transfection. Transfection experiments were carried out using human embryonic kidney cells HEK-293 cultured in DMEM supplemented with 1% penicillin and streptomycin, 1% glutamine, and 10% fetal bovine serum. Six well plates were seeded with 6×10^5 cells per well 24 h before transfection.

Lipofectamine transfection was performed according to Invitrogene transfection protocol. A 10 μL aliquot of 1 μg/μL pC4W-KCopGFP solution was dissolved in 40 μL of PBS. Then 10 μL of lipofectamine 2000 reagent was also dissolved in 40 μL of PBS. Then solutions were mixed dropwise by adding of lipofectamine to DNA. The resulting complex was allowed to stand at room temperature for 20 min. Cells were washed with DMEM without serum, and 1500 μL of culture medium per well was added. The complex solution was then added to the wells, and cells were incubated at 37 °C in 95% air/5% CO_2. After 24 h, media were replaced with fresh ones. Cells were cultured for

Table 1. Molecular Characteristics of Cationic wPPPDs

cationic dendrimer	number of phenylene groups	number of pyridinium groups		degree of alkylation β, %	
		N	N_{max}	elemental analysis (sulfur)	^{1}H NMR data
D_1^{6+}	10	6	6	99	98.4
D_1^{11+}	4	11	12	97	98.6
D_2^{14+}	28	14	18	77.8	78.0
D_2^{27+}	16	27	30	90	89.3
D_3^{54+}	40	54	66	81.8	81.1
D_4^{115+}	88	115	138	82.6	81.9

48 h, and then collected and examined for CopGFP fluorescence. Fluorescence intensity of CopGFP in transfected cells was determined using a FACSCalibur flow-cytometer (BD Immunocytometry Systems). For measurements, cells were collected by Trypsin-EDTA solution, washed with PBS and suspended in 1% phormaldehyde (ICN, USA) solution in PBS.

Transfection with wPPPD of the third generation (*dendrimer* D_3^{54+}) used 10 μL of pC4W-KCopGFP solution at 1 μg/μL dissolved in 50 μL of PBS and mixed with 175 μL of 6×10^{-3} mol/L dendrimer solution. The resulting complex solution was allowed to stand at room temperature for 20 min. Further procedures were performed as those with lipofectamine.

Results and Discussion

A series of cationic wPPPDs was synthesized as described in the Experimental Section. For the sake of convenience, hereafter the water-soluble dendrimer is denoted D_g^{N+}, where g is the dendrimer generation and N is a number of positively charged alkylated pyridinium groups that was calculated taking into account the degree of alkylation β. The D_g^{N+} sample notations, the amount of phenylene groups in their molecules, values of β, N, and N_{max} (assuming that the dendrimer is alkylated completely) are listed in Table 1.

These dendrimers denoted as D_1^{11+}, D_2^{27+}, D_3^{54+}, and D_4^{115+} constitute the family of wPPPDs being the first, second, third, and forth generations. The distribution of charges in the dendrimers was the same and determined by the arrangement of pyridyl groups in the molecules of parent PPPDs (Figure 1). In the samples D_1^{6+} and D_2^{14+}, there were half as many pyridinium cations as there are in D_1^{11+} and D_2^{27+}, respectively. The total number of aromatic groups in both pairs, i.e., D_1^{6+} and D_1^{11+} or D_2^{14+} and D_2^{27+}, was the same, yet the dendrimers D_1^{6+} and D_2^{14+} can be considered as hydrophobic analogues of the corresponding dendrimers D_1^{11+} and D_2^{27+}.

Formation and Stability of the DNA/wPPPD Complexes. DNA binding with wPPPD was monitored by ethidium bromide (EB) assay. The electrostatic binding of added cationic partner with DNA·EB complex resulted in conformational changes of the nucleic acid which eventually led to competitive displacement of the intercalated dye. The latter is accompanied by quenching of EB fluorescence.[67,68]

The titration of DNA·EB complex with solutions of dendrimers of different generations results in a linear decrease of fluorescence intensity I (Figure 2, curves 1−4). The values [+]/[−] plotted on the abscissa are the molar ratio of positively charged pyridinium moieties of the dendrimer to DNA phosphate groups. The fluorimetric curves differ in the slopes which reflect the efficacy of DNA binding with the cationic partner.[65] The least charged first generation D_1^{11+} is characterized by relatively low affinity to DNA (curve 1), whereas the consecutive 2-fold increase in a number of charges on passing to the second (curve 2) and then third generation (curve 3) considerably enhances the dendrimer affinity. However, for the fourth generation, the efficiency of the quenching noticeably decreases (curve 4).

Note that most if not all of studied to date highly charged linear polycations bound with DNA more efficiently, the

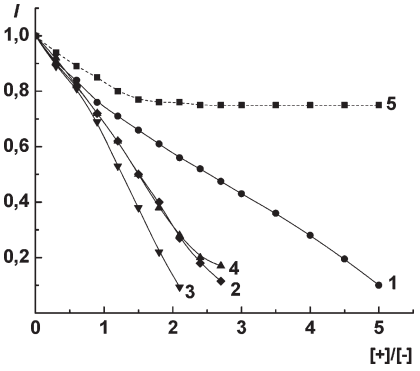

Figure 2. The curves of fluorimetric titration of DNA·EB complex with dendrimers of different generations: D_1^{11+} (1), D_2^{27+} (2), D_3^{54+} (3), D_4^{115+} (4), and D_1^{6+} (5). λ_{ex} 535 nm, λ_{em} 595 nm, [P] = 4×10^{-5} M, [EB]/[P] = 0.25, 0.01 M HEPES (pH = 7.2), 25 °C.

complete fluorescence quenching on titration of DNA·EB complex with the polycations solutions occurred at the ratio [+]/[−]≈1.[69] Presumably, the relatively inefficient binding of the dendrimers is to a great extent determined by the structural features of the interacting components, namely, the rigidity of DNA double helix and fixed spatial arrangement of charges in stiff wPPPD molecule.[57] Both these factors can hamper formation of the ion pairs. It is well documented[70] that four to six charged units arranged along the chain is quite sufficient for cooperative binding of oppositely charged flexible-chain linear polyions which bear a charge in each repeat unit. Evidently, to ensure cooperative interaction of DNA with wPPPDs, more charged groups in the dendrimer molecule are required. It can be concluded from the slopes of curves 1−3 of Figure 2 that the number of charges is certainly greater than 11, more than 27, and close to 54.

This assumption is supported by the decomposition profiles of the complexes in water-salt media (Figure 3). The curves were obtained by fluorimetric titration of the mixture of DNA, dendrimer and EB solutions with a concentrated (4 mol·L^{-1}) solution of sodium chloride as described elsewhere.[67] I/I_0 plotted on the ordinate is the ratio of fluorescence intensity of the mixture and DNA·EB solution, that were measured at the same salt concentration. In the case of the first generation dendrimer which binds with DNA least efficiently (Figure 2, curve 1), the addition of even the first portion of the salt results in a sharp increase in fluorescence intensity (Figure 3, curve 1) that subsequently continues to increase, indicating extensive decomposition of the DNA/D_1^{11+} complex. In spite of the DNA/D_2^{27+} complex is only slightly more stable (Figure3, curve 2), there is a small initial section in the curve characterized by insignificant growth of the intensity and only after that a sharp fluorescence increase occurs. The decomposition profile of the DNA/D_3^{54+} complex (curve 3) is clearly S-shaped, which is typical of decomposition curves of cooperative systems, specifically DNA complexes with flexible linear polyamines.[69] This result is

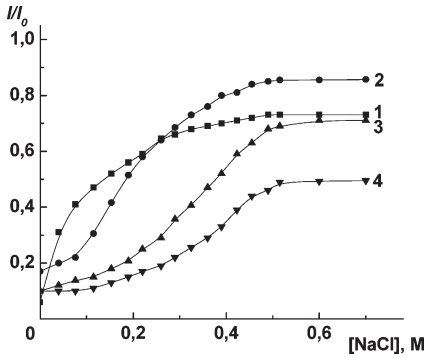

Figure 3. Dependences of relative fluorescence intensity of solutions of DNA complexes with dendrimers on salt concentration: D_1^{11+} (1), D_2^{27+} (2), D_3^{54+} (3), and D_4^{115+} (4). The conditions are the same as in the caption to Figure 2.

quite predictable in view of the high efficiency of D_3^{54+} binding with DNA (Figure 2, curve 3). The initial portion of curve 3 in Figure 3 is limited by the salt concentration of 0.22 mol·L^{-1}; i.e., this complex remains quite stable at physiological ionic strength (0.14 mol·L^{-1} NaCl).

Noteworthy that substitution of D_4^{115+} for D_3^{54+} (Figure 3, curves 3 and 4) does not result in a shortening of the initial part of the decomposition curve, as could be expected based on the data on efficacy of the dendrimers binding with DNA (Figure2, curves 3 and 4). Conversely, DNA complex with D_4^{115+} proved to be more resistant to the salt action and remains stable up to 0.25 mol·L^{-1} NaCl (Figure 3, curve 4). Apparently, D_4^{115+} molecule binds cooperatively with the nucleic acid and forms the greatest number of the ion pairs. However due to steric hindrance, this interaction does not involve all charged groups of the dendrimer (no more than one-third of them, as indicated by the slope of curve 4 in Figure 2). This finding is consistent with the data on potentiometric titration of DNA mixtures with polypropyleneimine dendrimers[57] that indicated the inaccessibility of amino groups located in the inner sphere of the high-generation dendrimers for electrostatic interaction with DNA.

On titration with a salt solution (Figure 3), the value $I/I_0 = 1$ corresponding to complete dissociation of the complex was attained in none of the systems. Most likely, the part of the ion pairs that are not destroyed even at relatively high ionic strength are stabilized by hydrophobic interactions of the dendrimer phenylene groups with some of the interior DNA bases which are nonpolar and therefore hyrdophobic.[71] This effect is pronounced in two opposite situations, namely, in the case of relatively weak electrostatic binding of D_1^{11+} (Figure 3, curve 1) and on cooperative electrostatic DNA interaction with D_4^{115+} that contains the greatest number of hydrophobic phenylene groups (curve 4). For dendrimers of the second (curve 2) and especially the third (curve 3) generations, this is manifested as I/I_0 values differing from unity and relatively slight slope of the destruction profiles.

Notice that DNA complexes with linear polyamine poly(*N*-ethyl-4-vinylpyridinium) bromide (PEVP) bearing alkylated pyridinium groups in repeat units, or with the third generation aliphatic polypropyleneimine dendrimer DAB-Am-16 having highly branched structure, can be destroyed completely by addition of the salt (Figure 4). Unlike the DNA/D_3^{54+} complex (Figure 4, curve 3), for PEVP (curve 1) and DAB-Am-16 (curve 2), the value $I/I_0 = 1$ is reached upon titration, and the curves slope steeply up. This difference confirms the important role of hydrophobic interactions in stabilization of the DNA/wPPPD complex which are conditioned by the presence of phenylene groups in the dendrimers.

The data obtained on studying the salt-induced dissociation of DNA complexes with more hydrophobic wPPPDs are an additional support of the stabilizing effect of the hydrophobic interactions (Figure5). By way of illustration, structural formulas of the hypothetically fully alkylated dendrimers of second generation D_2^{30+} and the corresponding hydrophobic analogue D_2^{18+} (note that the degree of alkylation is not 100%, see Table 1) are given below.

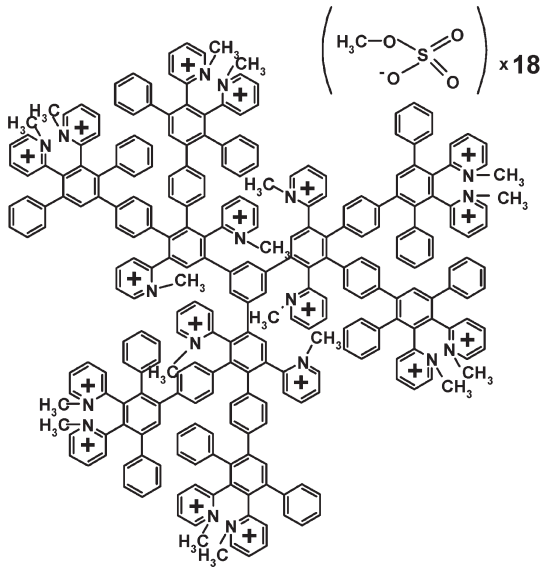

D_2^{18+}

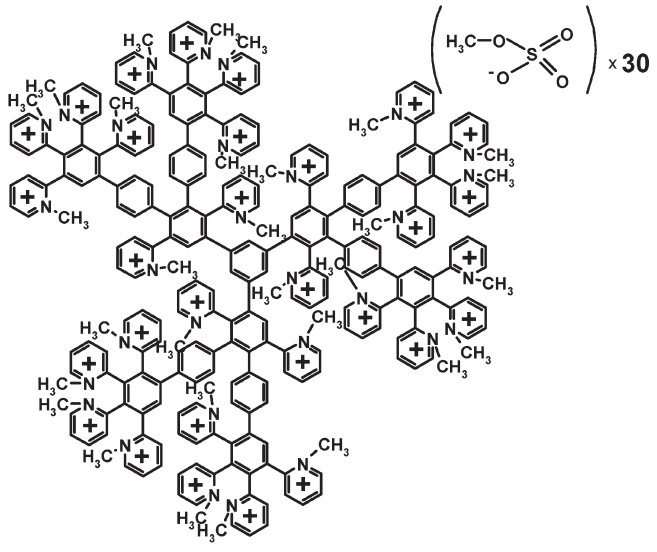

D_2^{30+}

Despite a number of positive charges in the hydrophobic analogue D_2^{14+} is halved, the decomposition of the DNA/D_2^{14+} complex (Figure 5, curve 2) occurs at a higher salt concentration as compared with the DNA/D_2^{27+} complex (curve 1), and the limiting value of I/I_0 is noticeably lower. Thus, the growth of a number of hydrophobic phenylene

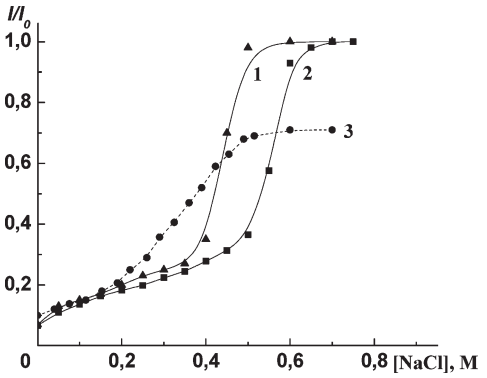

Figure 4. Dependences of relative fluorescence intensity of solutions of DNA complexes with linear polyamine PEVP (1), polypropyleneimine dendrimer DAB-Am-16 (2), and D_3^{54+} (3) on concentration of the added salt. The conditions are the same as in the caption to Figure 2.

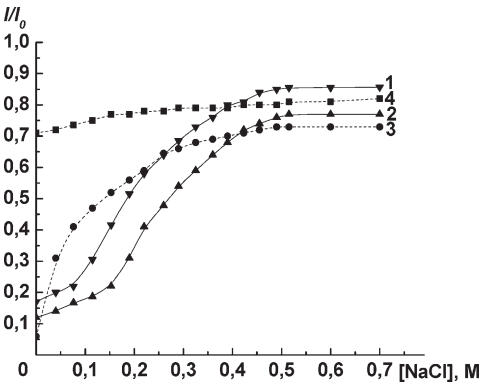

Figure 5. Dependences of relative fluorescence intensity of solutions of the DNA complexes with dendrimers of first and second generations (1, 3) and their hydrophobic analogues (2, 4) on salt concentration: D_2^{27+} (1), D_2^{14+} (2), D_1^{11+} (3), and D_1^{6+} (4). The conditions are the same as in the caption to Figure 2 .

groups in a dendrimer molecule attenuates the adverse salt action on the complex.

The fluorescence quenching caused by the titration of the DNA·EB complex with the least charged hydrophobic analogue D_1^{6+} was particularly inefficient being no more than 30% (Figure 2, curve 5). Rather low efficacy of the electrostatic binding results in arrangement of the decomposition profile of the DNA/D_1^{6+} system in the upper part of Figure 5 (curve 4), and hence, it is located above the profile of the first generation D_1^{11+} (curve 3). Nevertheless, the gently sloping curve 4 and relatively small limiting values of the fluorescence intensity indicate the resistance of this complex to the added salt. Besides, a slight opalescence of the DNA/D_1^{6+} mixture did not disappear in the course of the titration indicating the complex formation even at high salt concentrations.

All above findings are in favor of the complex stabilization by hydrophobic interactions. Obviously, a large number of wPPPDs phenylene groups capable of participation in hydrophobic interactions can be used, for example, for binding hydrophobic low-molecular-weight pharmaceutical agents. Such noncovalent immobilization appears to be the important step in the development of dual-purpose medicines in which the dendrimer acts both as the carrier of genetic material and a pharmaceutical agent.

Phase Separations in Solutions of the DNA/wPPPD Complexes. Phase behavior of the DNA/wPPPD mixtures was investigated by sedimentation assay and turbidimetry.

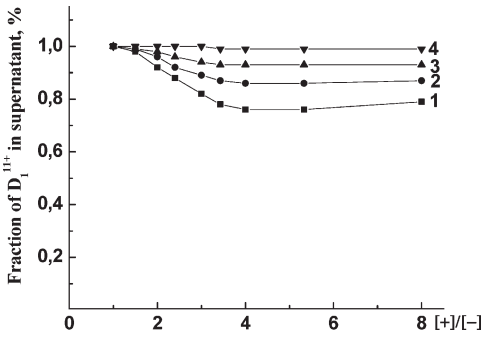

Figure 6. Fraction of D_1^{11+} in supernatant of the D_1^{11+} mixture with DNA of different composition, [+]/[−], determined at different concentrations of the added sodium chloride, M: 0 (1), 0.036 (2), 0.08 (3), and 0.115 (4). Other conditions are 11000 g, 10 min, λ = 310 nm, 2.4×10^{-4} M pyridinium groups, 0.01 M HEPES (pH = 7.2), 25 °C.

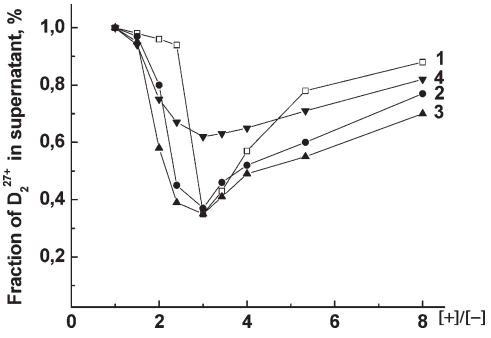

Figure 7. Fraction of D_2^{27+}remained in the supernatant of the D_2^{27+} mixture with DNA of the different composition, [+]/[−], determined at different concentrations of the added sodium chloride, M: 0 (1), 0.036 (2), 0.08 (3), and 0.115 (4). The conditions are the same as in the caption to Figure 6.

First generation D_1^{11+} which interacts with DNA inefficiently (curves 1 in Figure 2 and Figure 3) is not prone to precipitation upon mixing with the DNA solution. Formation of the insoluble complexes is noticeable only at [+]/[−] > 1 (Figure 6, curve 1). Further growth of a relative content of the dendrimer in the mixture is accompanied by insignificant accumulation of D_1^{11+} in the precipitate that comprises no more than 30% at 5-fold excess of the pyridinium cations. As might be expected, the addition of salt prevents formation of the insoluble complex because of a dissociation of the ion pairs which is particularly pronounced in this system (Figure 3, curve 1). An increase of the ionic strength results in the successive decrease of the D_1^{11+} fraction in the precipitate (Figure 6, curves 2, 3), and in 0.12 mol·L^{-1} NaCl practically all dendrimer molecules remain in the supernatant (curve 4).

The precipitation of the complex formed by the second generation is of greater intensity (Figure 7) that checks well with the ability of D_2^{27+} to bind more tightly with DNA, cf. curve 2 and curve 1 in Figure 3. In this case, the insoluble complex formation also occurs far from the equivalent content of the charged groups. Maximum precipitation is attained at 3-fold excess of the pyridinium groups (Figure 7, curve 1), i.e., at the ratio [+]/[−] $\approx$ 3 which corresponds to complete binding of the components as determined by the fluorescence quenching (Figure 2, curve 2). An increase of the charge ratio beyond the above value leads to a considerable decrease of the D_2^{27+} portion in the precipitate, and at 12-fold excess of the positive charges practically all the D_2^{27+}molecules remain in supernatant. This finding indicates formation of positively charged

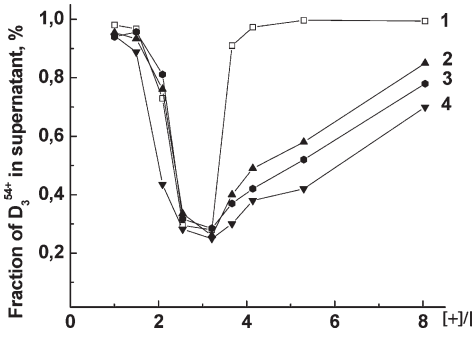

Figure 8. Fraction of D_3^{54+}remained in the supernatant of the D_3^{54+} mixture with DNA of the different composition, [+]/[−], determined at different concentrations of the added sodium chloride, M: 0 (1), 0.036 (2), 0.08 (3), and 0.115 (4) The conditions are the same as in the caption to Figure 6.

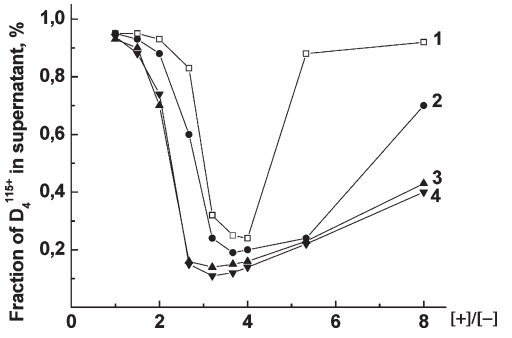

Figure 9. Fraction of D_4^{115+} in the supernatant of the D_4^{115+} mixture with DNA of the different composition, [+]/[−], determined at different concentrations of the added sodium chloride, M: 0 (1), 0.036 (2), 0.08 (3), and 0.115 (4). The conditions are the same as in the caption to Figure 6.

water-soluble nonstoichiometric polyelectrolyte complexes (NPECs) in which the dendrimer plays the role of the host lyophilizing component. Another argument in favor of this assumption is the sensitivity of right-hand part of the curve to the added salt. Unlike the DNA/D_1^{11+} system (Figure 6), the addition of sodium chloride in the DNA mixture with D_2^{27+} at [+]/[−] > 3 shifts the curve down (Figure 7, curves 2, 3) revealing formation and accumulation of the insoluble complex. It is well documented[72] that at a certain salt concentration, a great majority of soluble NPECs formed by linear oppositely charged polyions undergo the realignments that are accompanied by the formation of the insoluble complex. On further titration with the salt solution, when the ionic strength becomes sufficiently high, the precipitation is weakened due to the increasing contribution of another trend which acts in the opposite direction, i.e., the growth in complex solubility that is conditioned by successive descomposition of the ion pairs by the added salt. Accordingly, at [NaCl] > 0.08 mol·L^{-1} the precipitate is consecutively resolved (Figure 7, curve 4) that agrees well with decomposition profile of the DNA/D_2^{27+} system revealed by the fluorescence measurements (Figure3, curve 2).

The results of the assay of the third generation strongly suggest formation of positively charged NPEC if D_3^{54+} is at relatively large excess. The addition of the dendrimer solution at [+]/[-] > 3 is accompanied by sharp increase of D_3^{54+} portion in the supernatant (Figure 8, curve 1) that occurs with a much higher increment as compared with the run of analogous curve of the DNA/D_2^{27+} system (Figure 7, curve 1). Eventually, at [+]/[−] > 4 the insoluble complexes are not formed at all. In other words, D_3^{54+} exhibits a pronounced tendency to solubilize the insoluble products of the dendrimer interaction with DNA. These findings are in good agreement with the growth in capability of polypropyleneimine dendrimers to solubilize their complexes with DNA as one goes from younger to elder generations.[57] The addition of salt in the mixtures with large excess of D_3^{54+} also results in the formation of insoluble complexes (Figure 8, curves 2, 3) that proceeds in a wide range of salt concentrations (Figure 8, curve 4). A noticeable resolution of the precipitate occurred only at [NaCl] > 0.2 mol·L^{-1} (data not shown) that checks well with the pronounced tolerance of the DNA/D_3^{54+} complex to the decomposition by the salt (Figure 3, curve 3).

Back to Figure 7, one can see that at the early stages of the DNA titration with D_2^{27} (curve 1) practically all dendrimer molecules are retained in solution, an onset of the precipitation is only at 2.5-fold excess of the pyridinium groups. This suggests that at [+]/[−] < 2.5 water-soluble nonstoichiometric polyelectrolyte complexes with DNA as host lyophilizing component are formed. Just as in the case of the positively charged NPECs, i.e., in the mixture at [+]/[−] > 3, the addition of salt in the mixtures at [+]/[−] < 2.5 exerts the unfavorable influence on the soluble complexes (curves 2, 3). The same tendences are exhibited by the DNA/D_3^{54+} complex (Figure 8) with the only difference that in order to induce the phase separation a lesser excess of D_3^{54+} is required, [+]/[−] ≈ 1.8 (curve 1). This finding checks well with the growing efficacy of the DNA binding on passing from second to third generation (Figure 2, curve 2, 3). Water-soluble NPECs formed at [+]/[−] < 1.8 proved to be less sensitive to the added salt than the positively charged NPECs which contain a large excess of D_3^{54+}, cf. left- and right- hand parts of curves 2, 3, and 4 in Figure 8. The above difference in the salt sensitivity is inherent to NPECs formed by the host lyophilizing component which is either longer or shorter than the guest blocking component.[73] NPECs with the relatively long lyophilizing polyelectrolyte are thermodynamically more stable. In line with this trend, upon the addition of salt up to 0.08 mol·L^{-1} NaCl, the positively charged NPEC with short lyophilizing D_3^{54+} undergoes profound realignments and phase separations, whereas soluble NPEC with long lyophilizing DNA remains salt insensitive, cf. right- and left- hand parts of curves in Figure 8.

The same trends are exhibited by the DNA/D_4^{115+} mixtures. For the forth generation which forms the most stable complex (Figure 2, curve 4), the salt-induced shift of the left- and right- hand parts of the curve down is distinct (Figure 9). The addition of salt extends significantly the range of the precipitation. Most likely, formation of the insoluble complexes is facilitated by intermolecular hydrophobic interactions that are particularly pronounced due to the presence of numerous phenylene groups in the D_4^{115+} molecule. For the same reason, the forth generation dendrimer is not prone to form water-soluble NPECs on mixing of the component solutions. From comparison of the right-hand parts of curves 1 in Figure 8 and Figure 9 it follows that the 2-fold growth in a number of phenylene groups in the molecule on passing from the third to forth generation results in a noticeable weakening of the lyophilizing ability of the dendrimer.

In parallel with the sedimentation assay (Figure 6−9), phase separations in water-salt solutions of the DNA complexes with wPPPDs of different generations have been studied by turbidimetry. The data complemented each other and gave an accurate account of the regions corresponding to soluble complex formation. By the illustration, let us consider the results of turbidimetric titration of the soluble positively charged D_3^{54+}/DNA complexes with salt solution

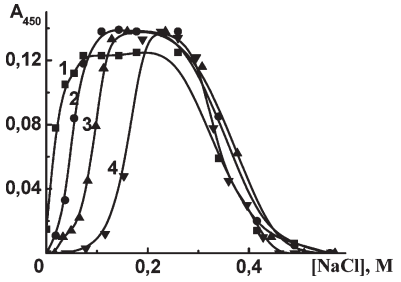

Figure 10. Turbidimetric titration curves of the D_3^{54+}/DNA mixtures of the different composition [+]/[−] with sodium chloride solution: [+]/[−] = 4 (1), 6 (2), 12 (3), and 24 (4). Other conditions are λ = 450 nm, $2*10^{-4}$M pyridinium groups, 0.01 M HEPES, pH = 7.2, 25 °C.

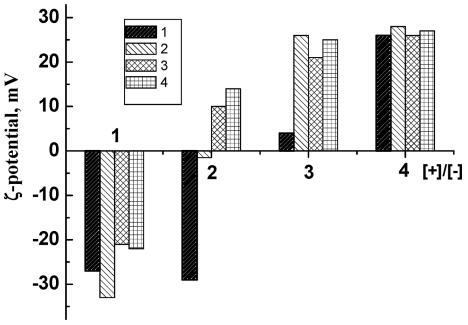

Figure 11. ζ-potential of the D_3^{54+} complexes with DNA(1), PMA, DP 1840 (2), PSS, DP 1710 (3) and PSS, DP 77 (4) formed at the different [+]/[−] ratios. Other conditions are 1.6×10^{-5} M pyridinium groups, 0.01 M TRIS buffer (pH = 9), 25 °C.

(Figure 10). The complexes of this kind are of particular interest for targeted transport of genetic material as the positive charge provides their binding with negatively charged cell membrane. Judging from the sedimentation assay, in the D_3^{54+}/DNA mixtures the insoluble complexes are not formed at [+]/[−] > 4 (Figure 8, curve 1). Accordingly, at [+]/[−] = 4 the turbidity of the system was quite close to zero (Figure 10, the initial point of curve 1). However, the addition of even a first portion of a titrant was accomplished with a sharp increase in the turbidity (curve 1) indicating poor stability of the soluble complex in water-salt media. As might be expected from the features of the NPEC solutions,[72] the stability increased with the rise in relative content of the host lyophilizing component (D_3^{54+}) in the mixture. The higher the [+]/[-] ratio, the more extended the initial part of the curve corresponding to the soluble complex (Figure 10, curves 1−4). Notice that at [+]/[−] = 24, the complex remained soluble even in 0.1 mol·L^{-1} NaCl solution (curve 4), i.e. at ionic strength close to physiological one (0.14 mol·L^{-1} NaCl). These findings are extremely encouraging for preparing of soluble dendriplexes stable under physiological pH and ionic strength.

Special consideration must be given to the revealed large shift of regions of the insoluble complex formation from the equimolar composition, [+]/[−] = 1. For a great majority of complexes formed by pairs of linear polyelectrolytes, the maximum precipitation occurred in the immediate vicinity of the charge neutralization. Moreover, this conclusion was confirmed by studying the DNA mixtures with polypropyleneimine dendrimers by turbidimetry[59] and sedimentation assay.[57] A different situation arises with the solutions of the DNA/wPPPD complexes. If no significance could be attached to weakly bound first generation which precipitated noticeably only at 5-fold excess of D_1^{11+} (Figure 6, curve 1), the precipitation of elder generations that bound with DNA cooperatively also needs a large excess of the dendrimer. Thus, maximum precipitation occurs at [+]/[−] ≈ 2.5 for D_3^{54+} (Figure 8, curve 1) and at [+]/[−] ≈ 3 both for D_2^{27+} (Figure 7, curve 1) and D_4^{115+} (Figure 9, curve 1).

The pronounced shift of the insoluble complex regions to the excess of the wPPPD charges in the mixture is attributable to inaccessibility of the pyridinium groups that are arranged in the inner part of the dendrimer for interaction with rigid double helix. In this particular case, the complete neutralization of the DNA phosphate groups which is essential for the formation of hydrophobic sequences in the complex needs the excess of the total number of the dendrimer positive charges. It is evident that the charges of the inaccessible pyridinium groups therewith remain uncompensated and hence, should lyophilize the complex. Judging from the data of the sedimentation assay (Figure 7−9), lyophilizing is not so pronounced to prevent the phase separations. The reduced solubilizing ability of wPPPDs can be explained by the presence of numerous hydrophobic phenylene groups in their molecules.

ζ-Potential Measurements. Positively charged pyridinium groups that are buried in the wPPPD molecule are not only inaccessible for electrostatic interaction with DNA, but they also do not contribute to the ζ potential of the complex species. Thus, in the DNA/D_3^{54+} mixtures, zero value of ζ-potential was accomplished at the [+]/[−] ratio slightly less than 3 (Figure 11, part 1). Notice that in the mixtures of D_3^{54+} with synthetic polyanion, e.g. sodium poly(methacrylate) (PMA) (Figure 11, part 2) or sodium poly(styrenesulfonate) (PSS) (parts 3 and 4), the reversal of sign of the surface charge occurred at lesser excess of the dendrimer, namely at [+]/[−] ≈ 2. This rise in efficacy of the binding is attributable to easier accessibility of the D_3^{54+} pyridinium groups to the flexible vinyl polyanions than to rigid double helix. It is of interest that on complexing of vinyl polyanions with polypropyleneimine dendrimers, all amino groups of the aliphatic dendrimers were involved in the electrostatic interaction,[57] reflecting the absence of steric hindrances. By contrast, in the molecules of stiff aromatic wPPPDs, a half of the pyridinium groups remains inaccessible for the synthetic polyanions regardless the degree of polymerization of the linear chains which was varied in a wide range, e.g., from 1710 to 77 repeat units of PSS (Figure 11, parts 3 and 4). In other words, even for relatively short PSS chains consisted of several tens of repeat units, the complexing was also hindered.

However the above tendency ceased to be true on passing from polyanions to oligomeric anions. Thus, the use of oligomeric PMA, DP 12 resulted in a noticeable decrease of the critical composition [+]/[−] (Figure 12, part 4), and for oligomeric PSS, DP 8, the surface charge of the complex species changes the sign in the immediate neighborhood of the equivalent point, [+]/[−] = 1 (Figure 12, part 5). The highest efficacy of binding of PSS, DP 8 could be determined by contribution of hydrophobic interactions between phenylene groups of the dendrimer and styrenesulfonate moieties that stabilize the complex. It should be particularly emphasized that the D_3^{54+} binding with longer but as yet relatively short chains PMA, DP 37 (Figure 12, 2) or PSS, DP 77 (Figure 12, 3) proceeds as inefficient as in the case of highly polymerized PMA and PSS anions (Figure 11, 2−4).

So, the substitution of oligomeric anions for polyanions results in a noticeable growth in the efficacy of the electrostatic interaction. Nothing of this sort has been established on complexing of either oppositely charged linear polyelectrolytes[70] or pairs of polymers bound with H-bonds.[74] Conversely, changing of the polymer partner to oligomeric one in

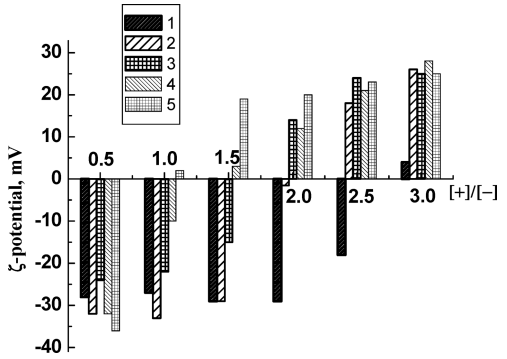

Figure 12. ζ-potential of the D_3^{54+} complexes with DNA(1), PMA_{37} (2), PSS_{77} (3), PMA_{12} (4) and PSS_8 (5) formed at the different [+]/[−] ratios. The conditions are the same as in the caption to Figure 11.

complexes of both types was accompanied by lowering of the binding efficiency. Accordingly, the revealed growth in a number of the ion pairs proves penetration of the oligomeric chains in the interior of the dendrimer and their interaction with pyridinium groups which are inaccessible for polyanions. The disclosed ability of cationic wPPPDs to prevent diffusion of relatively long negatively charged chains inside the dendrimer molecule and yet remain permeable to oligomeric anions strengthens the theory.[47] According to the employed computer simulation,[47] different types of complexes were observed to form depending on relative sizes of the molecules. For large dendrimers and short chains, the dendrimer encapsulates the chain and the chain collapses to a coil wrapped within the dendrimer. For relatively long linear polyelecrolyte, the chain has coiled near the dendrimer, but the rest of the chain remains extended. These findings could be used as the basis for the development of dendrimer vehicle to deliver cargo genetic materials, specifically oligonucleotides or siRNA. The penetration of the nucleotides in the inaccessible parts of the dendrimer and the corresponding growth in a number of the ion pairs should result in stabilization of the complex against the disintergrating action of the added salt. The latter is of crucial importance in transfection at physiological ionic strength. Besides, the oligonucleotides immobilized in the interior of the dendrimer might be reliably protected from undesired contacts with polymer compounds, specifically cell nucleases. Finally, the revealed influence of a degree of polymerization and hydrophobicity of the repeat units of the chains on the dendrimer permeability may form the basis for searching for hydrophobic pharmaceuticals suitable for the immobilization. The noncovalent immobilization appears to be a key point in the development of dual-purpose drugs mentioned above.

Dynamic Light Scattering Measurements. The measurements of the particle size in the D_3^{54+}/DNA mixtures by dynamic light scattering (Figure 13) agreed well with the sedimentation data and turbidimetry. As one would expect from the sedimentation assay (Figure 8, curve 1), at [+]/[−] < 4 a decrease in the relative content of D_3^{54+} resulted in formation of large micrometer-sized aggregates, whereas at [+]/[−] < 1.5 the particles again took on their nanoscale sizes of approximately 100 nm (Figure 13). The latter sustains formation of soluble negatively charged NPEC with DNA as lyophilizing host polyelectrolyte. The sizes of the soluble positively charged NPECs determined at [+]/[−] > 4 were 110 ± 10 nm as well. This suggests that the particles of the soluble complexes are nonaggregated and could penetrate into the cell by endocytosis since their hydrodynamic diameter D_h does not exceed the critical value of 150 nm.[75]

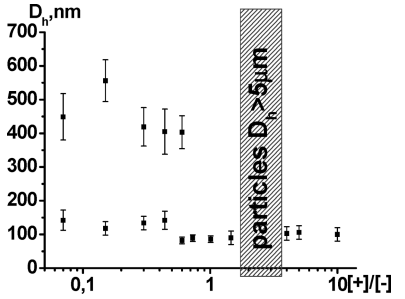

Figure 13. Hydrodynamic diameter of particles formed in the solutions of $D_3^{54+}$and DNA of the different [+]/[−] composition. Other conditions are [P] = 9×10^{-5} M, 0.01 M HEPES buffer (pH = 7.2), 25 °C.

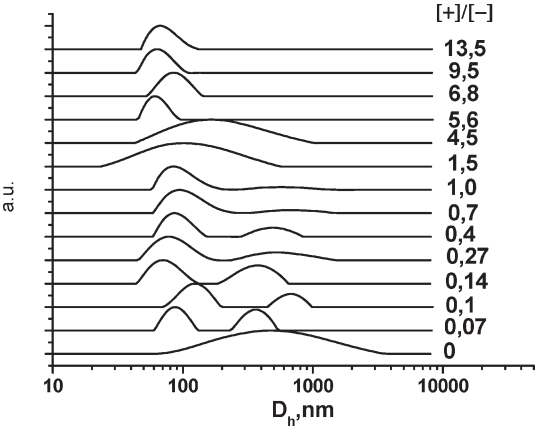

Figure 14. Intensity weighted distribution function for the mixtures of the DNA solution with D_3^{54+} at the different [+]/[−] ratios of the components. The angle α = 90°; other conditions were the same as in the caption to Figure 13.

Closer examination of the dynamic light-scattering data, specifically the left part of Figure 13 allows one to arrive at one more important conclusion. For the sake of convenience, the data of Figure13 are depicted in Figure14 as a function of the particle distribution. In solution of free DNA (Figure14, [+]/[−] = 0), only one relatively broad peak is recorded that corresponds to the translational mode of the molecules of a mean hydrodynamic diameter about 500 nm. On addition of even the first portion of D_3^{54+} ([+]/[−] = 0.07), a second peak appeared which coexists with the first peak and is related to significantly smaller particles of the hydrodynamic diameter, of not more than 100 nm. These two populations of the particles are maintained in a wide range of the mixture composition. In this region, the growth in relative content of the dendrimer is accompanied by both a decrease in area of the peak corresponding to large species and an increase of the amplitude of the peak related to compact particles to the extent of complete disappearance of the former species at [+]/[−] = 1.35. On further growth in the dendrimer content, the size of the compact particles increases with the broadening of their distribution and eventually at certain value of the composition, [+]/[−] = 2.7, the micrometer-sized aggregates are formed. It is seen that the sizes of compact particles coexisting with the large ones virtually coincide with the sizes of soluble NPECs formed on the left and right sides from the heterogeneous region. The size of the large species, D_h = 450 ± 50 nm, is comparable with the diameter of free DNA measured under the same conditions.

According to the reported data on DLS measurements of DNA in solutions,[76,77] at the angles larger than 57°, the

correlation function can exhibit two or more relaxation modes, reflecting internal dynamics in addition to the translational diffusion of the double helix. So at the first glance, it is not inconvincible that the second mode corresponding to relatively small hydrodynamic diameters is conditioned by the internal dynamics. But in this particular case, the above mode should eventually disappear on the growth in relative content of D_3^{54+} in the mixture due to the DNA compaction (no internal modes are detected for homogeneous hard spheres[78]). Because in the experiments just the reverse tendency is observed (i.e., the increase in the peak amplitude), it is reasonable to assign the peak to compact species of the D_3^{54+}/DNA complex.

An argument in favor of the species of two populations is the data on the high-speed sedimentation assay. The patterns of the D_3^{54+}/DNA mixtures of the composition [+]/[−] < 1.35 evidence relatively slow and much more quickly moving fractions. The coefficient of sedimentation S_c of the slow fraction practically coincided with $S_c = 16$ of free DNA, and the portion of these particles successively decreased with the growth in the dendrimer content to the extent of their disappearance. The latter occurred at the same charge ratio that corresponds to the transfer from bimodal to unimodal distribution on the DLS patterns (Figures 13 and 14). The sedimentation of coexisting particles proved to be too fast to provide the measurements of the sedimentation coefficient. Judging from the high values of the [+]/[−] ratio corresponding to the above-mentioned transformation (Figures 13, 14), the content of the dendrimer in the soluble D_3^{54+}/DNA complex is relatively high and hence, the neutralization of the DNA phosphate groups by the added charged dendrimer is profound. This suggests the distinct compaction of the complex particles and relatively low charge density on their surface. Both these assumptions are in agreement with the fast moving of the complex particles on the sedimentation.

Notice, the bimodal distribution in the system was virtually not changed in time. Thus, the size of the particles in the D_3^{54+}/DNA mixtures of the composition [+]/[−] = 0.14 measured in a half an hour after the preparation (Figure15, curve 1) was nearly the same during 24 h incubation at the same temperature (curve 2), whereas the size of large particles decreased but rather insignificantly. These findings imply that the revealed bimodal distribution is hardly the result of kinetic hindrances that occurs on addition of a relatively concentrated solution of one component to the dilute solution of another one. Most likely, the reason is thermodynamic by nature and conditioned by a decrease in Gibbs free energy of the system on "loading" of a limited number of DNA molecules by numerous molecules of the positively charged partner. The complexing is accompanied by formation of the compact species which inevitably results in destruction of unique conformation of bound double helices. In the systems with two particle populations, the coexisting practically unbound DNA molecules maintain their rigid highly ordered conformation that reduces to minimum the thermodynamically unfavorable changes caused by interpolyelecrolyte interactions.

The detailed elucidation of the reasons of the above phenomenon is out of the scope of the current paper and evidently merits special consideration as similar event (bimodal distribution) was reported on studying DNA mixtures with cationic surfactants[79−82] or PAMAM dendrimers.[83]

AFM Study. An advantage of the AFM method is that biological molecules can be imaged without the use of contrast enhancement techniques and the number of papers has been focused on the application of this method toward

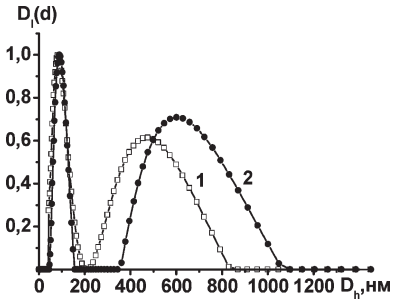

Figure 15. Intensity weighted distribution function for the D_3^{54+}/DNA mixture of the [+]/[−] = 0.14 composition measured in a half an hour (1) and after 24 h incubation (2). The angle $\alpha = 90°$; other conditions were the same as in the caption to Figure 13.

biological and polymeric systems.[84−91] The most common substrate for DNA imaging is mica due to its smooth surface. As mica is negatively charged, the presence of a divalent cation, either in solution or accessible to DNA on the mica substrate, greatly improves the DNA adsorption.[92] In this work $MgCl_2$ was used as a source of the positively charged Mg^{2+} ions to induce cross-bridges between negatively charged mica surface and the negative phosphate groups of DNA.

AFM image of linear DNA deposited from HEPES solution containing 1 mM of $MgCl_2$ is shown in Figure 16a. The DNA molecules are mostly seen as elongated individual strands. The height of DNA is 0.7 ± 0.2 nm, which is lower that the value of ~2 nm known for B-DNA.[93] The reasonable explanation for this fact is compression of DNA as a result of scanning by an AFM tip along with electrostatic interaction between a DNA sample and a substrate.

We were especially interested in elucidating the morphology of soluble wPPPD/DNA complexes formed at a large excess of the positively charged dendrimer. The positive charge of the complexes is a requirement for effective transfection.[94−96] However, because strong electrostatic adsorption of a positively charged complex on negatively charged mica might distort an AFM image of the D_3^{54+}/DNA complex, it was measured on a HOPG surface (uncharged) to minimize the influence of the interaction with the surface on complex morphology.

The AFM image of the complex formed at a charge ratio [+]/[−] = 12 (Figure 16b) shows formation of the "necklace" like aggregates densely populated with "beads". The average height of the aggregates is higher than that of bare DNA (Figure 16a). On the basis of the AFM data, we propose the structural model for the DNA/dendrimer complex according to which the resulting complex is a chain completely "decorated" with spheres, each of which is undercharged (positively charged). If this is the case, due to a charge density mismatch the part of dendrimer positive charges located in the interior of the stiff dendrimer sphere remains noncompensated providing the complex solubility. This model is in agreement with a model developed by Schiessel who considered complexes formed between positively charged hard sphere macroions and a persistent linear PE.[38] Additionally, it is evident from the AFM data that the complex consists of several DNA strands linked through a dendrimer junction. The major part of the HOPG surface is covered, most probably, by isolated dendrimers (or dendrimer aggregates) which might be attracted to the nonpolar HOPG due to hydrophobic interactions. Here the structure of the complex (Figure 16b) is different from that of polyelectrolyte complexes formed between DNA and various cationic compacting agents such as polymeric or multivalent counterions

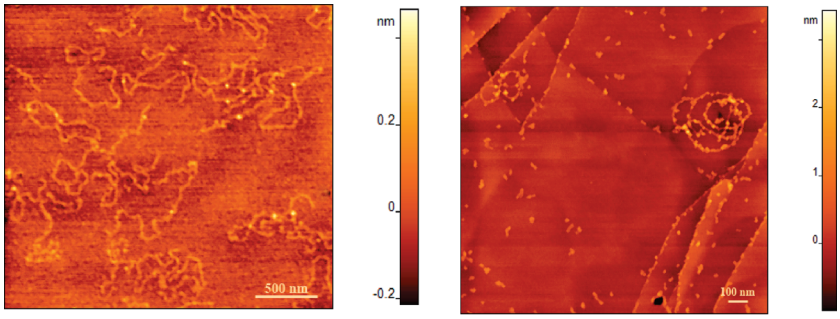

Figure 16. AFM images of (a) linear pC4W-KCopGFP DNA on a mica and (b) complexes formed by linear DNA pC4W-KCopGFP and D_3^{54+} on a HOPG at a charge ratio [+]/[−] = 12; c(DNA) = 0.01 g L^{-1}.

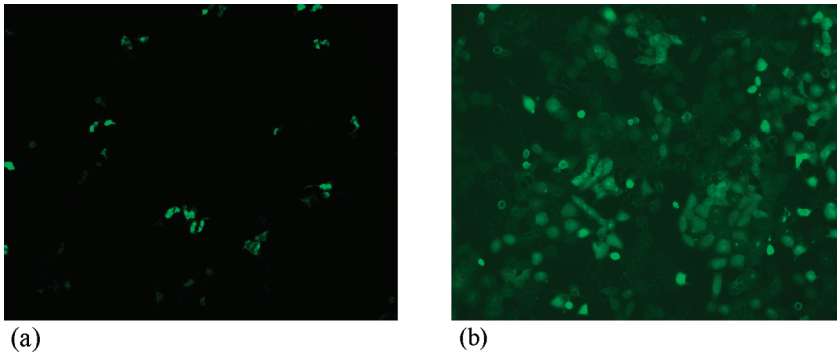

Figure 17. Transfection of HEK-293 cells with dendrimer D_3^{54+} (a) and with lipofectamine 2000 reagent (b). Fluorescence microscopy, magnification 150 times.

reported by others.[91,97,98] In the recent paper[91] on complex formation between DNA and cylindrical brushes and a PAMAM dendrimer, the aggregates with a core comprising at least several complexed polycation molecules surrounded by an open DNA corona (resulting in a flower-like structure) have been reported However, it is worth noting that the experiments were performed with the excess of negatively charged DNA. The similar flower-like structures induced by divalent counterions were reported in ref 84. In the opposite case, at the excess of positively charged polymeric counterions the formation of big aggregates of compacted DNA has been documented, however the morphology of such complexes was not clarified.[91] Thus, no morphology similar to that reported in this paper has been observed for positively charged DNA/dendrimer polyelectrolyte complexes.

In Vitro Cell Transfection with Dendrimer D_3^{54+}. The experiments on transfection of human embryonic kidney cells HEK-293 with expression plasmid pC4W-KCopGFP have been performed using D_3^{54+} and, in comparison, Lipofectamine 2000 reagent as described in detail in the Experimental Section. The distinct fluorescence of the cell (Figure17a) evidenced cell transfection by the dendrimer that was 20 times lower in efficiency as compared with one of the most efficient transfection agent lipofectamine 2000 (Figure17b). Noteworthy that viability of the cells in both experiments remained rather high proving low toxicity of the dendrimer.

The modest efficiency of wPPPD vector might be due to absence of the so-called "proton-sponge" effect. Behr[99] and others introduced the concept of the "proton sponge" and hypothesized that polymers with buffering capacities between 7.2 and 5.0, such as polyethylenimine (PEI) and some dendrimers could buffer the endosome and potentially induce its rupture due to a high osmotic pressure thus providing transfection effeciency. Additionally, the effect of chain length on transfection efficiency can also play a role.[100] The exhaustive alkylation of wPPPDs almost eliminates the possibility to absorb more protons inside endocytic vesicles. However, decrease in alkylation degree might lead to improving transfection efficiency as it was reported for vectors based on partly quaternized poly(4-vinylpyridine)s.[101] Such a study will be a focus of our further research.

All above-mentioned findings imply that wPPPD molecules are applicable for model investigations on the elucidating of structure−function correlations of the aromatic dendrimer vehicles.

Conclusion

We studied the interaction of calf thymus DNA with cationic water-soluble aromatic dendrimers of different generations and hydrophobicity. The DNA/wPPPD polyelectrolyte complexes proved to be particularly stable against the disintegrating action of the added salt due to a significant contribution of hydrophobic interactions provided by phenylene moieties. The inaccessibility of positively charged groups situated in the inner area of wPPPD molecule not only for rigid double helix (as it was ascertained earlier by potentiometric titration of DNA mixture with flexible polypropyleneimine dendrimers[57]) but also for flexible synthetic polyanions has been established. The later feature was assign to steric hindrances conditioned by wPPPD stiffness. It is reasonable to assume that the inaccessibility of the interior of the rigid aromatic dendrimers gives rise to the specific conformation of the resulting complexes which is responsible for the distinct ability of wPPPDs to form negatively or positively charged water-soluble polyelectrolyte complexes with DNA. The positively charged complexes formed at large excess of the pyridinium groups remained soluble at ionic strength close to physiological one. This finding could be particularly important for development of

wPPPD vehicles suitable for delivering of physiologically active compounds to the cell. The presence in the dendrimers of a large number of phenylene groups capable to participate in hydrophobic interactions can be used, for example, for binding hydrophobic low-molecular-weight pharmaceutical agents. Such noncovalent immobilization appears to be the important step in the development of dual-purpose medicines in which the dendrimer acts both as the carrier of genetic material and a pharmaceutical agent.

Acknowledgment. We thank Dr. T. V. Laptinskaya, Department of Physics, Moscow State University and Professor V. V. Vasilevskaya, A. N. Nesmeyanov Institute of Organoelement Compounds RAS, for fruitful discussions as well as Professor I. V. Yaminsky, Chemistry Department, Moscow State University, Moscow, Russia for practical advice on the AFM study. Financial support from the Russian Foundation for Basic Research (Projects 07-03-00220 and 07-03-00228) is gratefully acknowledged.

References and Notes

(1) Buhleier, E.; Wehner, W.; Voegtle, F. *Synthesis* **1978**, 155–158.
(2) Tomalia, D. A.; Baker, H.; Dewald, J. R.; Hall, M.; Kallos, G.; Martin, S.; Roeck, J.; Ryder, J.; Smith, P. *Polym. J.* **1985**, *17*, 117–132.
(3) Tomalia, D. A.; Baker, H.; Dewald, J.; Hall, M.; Kallos, G.; Martin, S.; Roeck, J.; Ryder, J.; Smith, P. *Macromolecules* **1986**, *19*, 2466–2468.
(4) Newkome, G. R.; Yao, Z. Q.; Baker, G. R.; Gupta, V. K. *J. Org. Chem.* **1985**, *50*, 2003–2006.
(5) Tomalia, D. A.; Durst, H. D. *Top. Curr. Chem.* **1993**, *165*, 193–313.
(6) Newkome, G. R.; Moorefield, C. N.; Voegtle, F., *Dendritic Molecules: Concept, Synthesis, Perspectives*; VCH.: Weinheim, Germany, 1996.
(7) Zeng, F.; Zimmerman, S. C. *Chem. Rev.* **1997**, *97*, 1681–1712.
(8) Balzani, V.; Ceroni, P.; Maestri, M.; Saudan, C.; Vicinelli, V., *Top. Curr. Chem.* **2003**, *228*, 159−191.
(9) Berresheim, A. J.; Muller, M.; Mullen, K. *Chem. Rev.* **1999**, *99*, 1747–1785.
(10) Bosman, A. W.; Janssen, H. M.; Meijer, E. W. *Chem. Rev.* **1999**, *99*, 1665–1688.
(11) Majoral, J. P.; Caminade, A. M. *Chem. Rev.* **1999**, *99*, 845–880.
(12) Vogtle, F.; Gestermann, S.; Hesse, R.; Schwierz, H.; Windisch, B. *Prog. Polym. Sci.* **2000**, *25*, 987–1041.
(13) Grayson, S. M.; Frechet, M. *J. Chem. Rev.* **2001**, *101*, 3819–3867.
(14) Esumi, K. *Top. Curr. Chem.* **2003**, *227*, 31–52.
(15) Tomalia, D. A. *Prog. Polym. Sci.* **2005**, *30* (3−4), 294–324.
(16) Rajadurai, M. S.; Shifrina, Z. B.; Kuchkina, N. V.; Rusanov, A. L.; Muellen, K. *Usp. Khim.* **2007**, *76*, 821–838.
(17) Astruc, D.; Ornelas, C.; Ruiz, J. *Acc. Chem. Res.* **2008**, *41*, 841–856.
(18) Frechet, J.; Tomalia, D., *Dendrimers and other dendritic polymers*; Wiley: Chichester, U.K., 2001.
(19) Balzani, V.; Campagna, S.; Denti, G.; Juris, A.; Serroni, S.; Venturi, M. *Acc. Chem. Res.* **1998**, *31*, 26–34.
(20) van Heerbeek, R.; Kamer, P. C. J.; van Leeuwen, P. W. N. M.; Reek, J. N. H. *Chem. Rev.* **2002**, *102*, 3717–3756.
(21) Newkome, G. R.; He, E. F.; Moorefield, C. N. *Chem. Rev.* **1999**, *99*, 1689–1746.
(22) Duncan, R.; Izzo, L. *Adv. Drug Delivery Rev.* **2005**, *57*, 2215–2237.
(23) Dufes, C.; Uchegbu, I. F.; Schatzlein, A. G. *Adv. Drug Delivery Rev.* **2005**, *57*, 2177–2202.
(24) Thomas, T. P.; Majoros, I. J.; Kotlyar, A.; Kukowska-Latallo, J. F.; Bielinska, A.; Myc, A.; Baker, J. R. *J. Med. Chem.* **2005**, *48*, 3729–3735.
(25) Thomas, T. P.; Ye, J. Y.; Chang, Y. C.; Kotlyar, A.; Cao, Z.; Majoros, I. J.; Norris, T. B.; Baker, J. R. *J. Biomed. Opt.* **2008**, *13*, 1.
(26) Caruthers, S. D.; Wickline, S. A.; Lanza, G. M. *Curr. Opin. Biotechnol.* **2007**, *18* (1), 26–30.
(27) Wolinsky, J. B.; Grinstaff, M. W. *Adv. Drug Delivery Rev.* **2008**, *60*, 1037–1055.
(28) Goldberg, M.; Langer, R.; Jia, X. Q. *J. Biomater. Sci., Polym. Ed.* **2007**, *18*, 241–268.
(29) Svenson, S.; Tomalia, D. A. *Adv. Drug Delivery Rev.* **2005**, *57*, 2106–2129.
(30) Mateescu, E. M.; Jeppesen, C.; Pincus, P. *Europhys. Lett.* **1999**, *46*, 493–498.
(31) Netz, R. R.; Joanny, J. F. *Macromolecules* **1999**, *32*, 9026–9040.
(32) Kunze, K. K.; Netz, R. R. *Phys. Rev. Lett.* **2000**, *85*, 4389–4392.
(33) Kunze, K. K.; Netz, R. R. *Phys. Rev. E* **2002**, *66*, 011918–011946.
(34) Nguyen, T. T.; Shklovskii, B. I. *J. Chem. Phys.* **2001**, *115*, 7298–7308.
(35) Nguyen, T. T.; Shklovskii, B. I. *Phys. A: Stat. Mech. Its Appl.* **2001**, *293* (3−4), 324–338.
(36) Nguyen, T. T.; Shklovskii, B. I. *J. Chem. Phys.* **2001**, *114*, 5905–5916.
(37) Schiessel, H. *Macromolecules* **2003**, *36*, 3424–3431.
(38) Schiessel, H.; Bruinsma, R. F.; Gelbart, W. M. *J. Chem. Phys.* **2001**, *115*, 7245–7252.
(39) Schiessel, H.; Rudnick, J.; Bruinsma, R.; Gelbart, W. M. *Europhys. Lett.* **2000**, *51*, 237–243.
(40) Grosberg, A. Y.; Nguyen, T. T.; Shklovskii, B. I. *Rev. Mod. Phys.* **2002**, *74*, 329–345.
(41) Wallin, T.; Linse, P. *J. Phys. Chem.* **1996**, *100*, 17873–17880.
(42) Wallin, T.; Linse, P. *Langmuir* **1996**, *12*, 305–314.
(43) Wallin, T.; Linse, P. *J. Phys. Chem. B* **1997**, *101*, 5506–5513.
(44) Wallin, T.; Linse, P. *J. Chem. Phys.* **1998**, *109*, 5089–5100.
(45) Jonsson, M.; Linse, P. *J. Chem. Phys.* **2001**, *115*, 10975–10985.
(46) Jonsson, M.; Linse, P. *J. Chem. Phys.* **2001**, *115*, 3406–3418.
(47) Welch, P.; Muthukumar, M. *Macromolecules* **2000**, *33*, 6159–6167.
(48) Lyulin, S. V.; Darinskii, A. A.; Lyulin, A. V. *Macromolecules* **2005**, *38*, 3990–3998.
(49) Lyulin, S. V.; Vattulainen, I.; Gurtovenko, A. A. *Macromolecules* **2008**, *41*, 4961–4968.
(50) Maiti, P. K.; Bagchi, B. *Nano Lett.* **2006**, *6*, 2478–2485.
(51) Qamhieh, K.; Nylander, T.; Ainalem, M.-L. *Biomactomolecules* **2009**, *10*, 1720–1726.
(52) Kabanov, V. A.; Sergeyev, V. G.; Pyshkina, O. A.; Zinchenko, A. A.; Zezin, A. B.; Joosten, J. G. H.; Brackman, J.; Yoshikawa, K. *Macromolecules* **2000**, *33*, 9587–9593.
(53) Chen, W.; Turro, N. J.; Tomalia, D. A. *Langmuir* **2000**, *16*, 15–19.
(54) Mitra, A.; Imae, T. *Biomacromolecules* **2004**, *5*, 69.
(55) Ottaviani, M. F.; Furini, F.; Casini, A.; Turro, N. J.; Jockusch, S.; Tomalia, D. A.; Messori, L. *Macromolecules* **2000**, *33*, 7842.
(56) Ottaviani, M. F.; Sacchi, B.; Turro, N. J.; Chen, W.; Jockush, S.; Tomalia, D. A. *Macromolecules* **1999**, *32*, 2275.
(57) Kabanov, V. A.; Zezin, A. B.; Rogacheva, V. B.; Gulyaeva, Z. G.; Zansochova, M. F.; Joosten, J. G. H.; Brackman, J. *Macromolecules* **1999**, *32*, 1904–1909.
(58) Bielinska, A. U.; KukowskaLatallo, J. F.; Baker, J. R. *Biochim. Biophys. Acta: Gene Struct. Expression* **1997**, *1353* (2), 180–190.
(59) Kabanov, V. A.; Zezin, A. B.; Rogacheva, V. B.; Gulyaeva, Z. G.; Zansochova, M. F.; Joosten, J. G. H.; Brackman, J. *Macromolecules* **1998**, *31*, 5142–5144.
(60) Shifrina, Z. B.; Rajadurai, M. S.; Firsova, N. V.; Bronstein, L. M.; Huang, X.; Rusanov, A. L.; Muellen, K. *Macromolecules* **2005**, *38*, 9920–9932.
(61) Brocorens, P.; Zojer, E.; Cornil, J.; Shuai, Z.; Leising, G.; Mullen, K.; Bredas, J. L. *Synth. Met.* **1999**, *100*, 141.
(62) Shifrina, Z. B.; Kuchkina, N. V.; Rusanov, A. L.; Izumrudov, V. A. *Dokl. Chem.* **2007**, *416*, 213–216.
(63) Waring, M. J. *J. Mol. Biol.* **1965**, *13* (1), 269.
(64) Olins, D. E.; Olins, A. L.; von Hippel, P. H. V. N. P. *J. Mol. Biol.* **1967**, *24* (2), 157.
(65) Izumrudov, V. A.; Zhiryakova, M. V.; Kudaibergenov, S. E. *Biopolymers* **1999**, *52* (2), 94–108.
(66) Starodubtsev, S. G.; Kirsh, Y. E.; Kabanov, V. A. *Eur. Polym. J.* **1977**, *10*, 739–742.
(67) Izumrudov, V. A.; Zezin, A. B.; Kargov, S. I.; Zhiryakova, M. V.; Kabanov, V. A. *Dokl. Akad. Nauk* **1995**, *342*, 626–629.
(68) Bronich, T. K.; Nguyen, H. K.; Eisenberg, A.; Kabanov, A. V. *J. Am. Chem. Soc.* **2000**, *122*, 8339–8343.
(69) Izumrudov, V. A.; Zhiryakova, M. V. *Macromol. Chem. Phys.* **1999**, *200*, 2533–2540.
(70) Tsuchida, E.; Abe, K. *Adv. Polym. Sci.* **1982**, *45*, 1–119.
(71) Martin, R. B., *Introduction to Biophysical Chemistry*. McGraw-Hill Book Company: NewYork, 1964.
(72) Kabanov, V. A.; Zezin, A. B. *Pure Appl. Chem.* **1984**, *56*, 343–354.
(73) Izumrudov, V. A.; Paraschuk, V. V.; Sybachin, A. V. *J. Drug Deliv. Sci. Technol.* **2006**, *16*, 267–274.

(74) Papisov, I. M.; Litmanovich, A. A. *Adv. Polym. Sci.* **1989**, *90*, 139–179.
(75) Kabanov, A. V.; Szoka, F. C.; Seymour, L. W., In *Self-assembling Complexes for Gene Delivery. From Laboratory to Clinical Trial* Kabanov, A. V., Felgner, P. L., Seymour, L. W., Eds. John Wiley & Sons: Chichester, U.K., 1998; pp 197−218.
(76) Sorlie, S. S.; Pecora, R. *Macromolecules* **1988**, *21*, 1437–1449.
(77) Sorlie, S. S.; Pecora, R. *Macromolecules* **1990**, *23*, 487–497.
(78) Burchard, W. In *Light Scattering. Principles and developments*; Brown, W., Ed.; Oxford University Press: Oxford, U.K., 1996; pp 439−476.
(79) Mel'nikov, S. M.; Khan, M. O.; Lindman, B.; Jonsson, B. *J. Am. Chem. Soc.* **1999**, *121*, 1130–1136.
(80) Dias, R. S.; Lindman, B.; Miguel, M. G. *J. Phys. Chem. B* **2002**, *106*, 12600–12607.
(81) Melnikov, S. M.; Sergeyev, V. G.; Yoshikawa, K. *J. Am. Chem. Soc.* **1995**, *117*, 2401–2408.
(82) Melnikov, S. M.; Sergeyev, V. G.; Yoshikawa, K. *J. Am. Chem. Soc.* **1995**, *117*, 9951–9956.
(83) Orberg, M. L.; Schillen, K.; Nylander, T. *Biomacromolecules* **2007**, *8*, 1557–1563.
(84) Li, Y.; Yildiz, U. H.; Mullen, K.; Grohn, F. *Biomacromolecules* **2009**, *10*, 530–540.
(85) Dubrovin, E. V.; Drygin, Y. F.; Novikov, V. K.; Yaminsky, I. V. *Nanomed: Nanotechnol. Biol. Med.* **2007**, *3* (2), 128–131.
(86) Dubrovin, E. V.; Staritsyn, S. N.; Yakovenko, S. A.; Yaminsky, I. V. *Biomacromolecules* **2007**, *8*, 2258–2261.
(87) Vinogradova, O. I.; Lebedeva, O. V.; Vasilev, K.; Gong, H. F.; Turiel, J.; Kim, B. S. *Biomacromolecules* **2005**, *6*, 1495–1502.
(88) Volcke, C.; Pirotton, S.; Grandfils, C. H.; Humbert, C.; Thiry, P. A.; Ydens, I.; Dubois, P.; Raes, M. *J. Biotechnol.* **2006**, *125*, 11–21.
(89) Zheng, J.; Li, Z.; Wu, A.; Zhou, H. *Biol. Phys. Chem.* **2003**, *104*, 37–43.
(90) Maurstad, G.; Stokke, B. T. *Biopolymers* **2004**, *74*, 199–213.
(91) Storkle, D.; Duschner, S.; Heimann, N.; Maskos, M.; Schmidt, M. *Macromolecules* **2007**, *40*, 7998–8006.
(92) Bezanilla, M.; Manne, S.; Laney, D. E.; Lyubchenko, Y. L.; Hansma, H. G. *Langmuir* **1995**, *11*, 665–659.
(93) Nelson, D. L.; Cox, M. M. *Lehinger. Principles of Biochemistry*, 3rd ed.; Wroth Publishers: New York, 2000.
(94) Takeuchi, K.; Ishihara, M.; Kawaura, C.; Noji, M.; Furuno, T.; Nakanishi, M. *FEBS Lett.* **1996**, *397* (2−3), 207–209.
(95) Zelphati, O.; Szoka, F. C. *Pharm. Res.* **1996**, *13*, 1367–1372.
(96) Labhasetwar, V. *Curr. Opin. Biotechnol.* **2005**, *16*, 674–680.
(97) Fang, Y.; Hoh, J. H. *J. Am. Chem. Soc.* **1998**, *120*, 8903–8909.
(98) Choi, J. S.; Joo, D. K.; Kim, C. H.; Kim, K.; Park, J. S. *J. Am. Chem. Soc.* **2000**, *122*, 474–480.
(99) Behr, J. P. *Chimia* **1997**, *51* (1−2), 34–36.
(100) Deng, R.; Yue, Y.; Jin, F.; Chen, Y.; Kung, H.-F.; Lin, M. C. M.; Wu, C. *J. Controlled Release* **2009**, *140*, 40–46.
(101) San Juan, A.; Letourneur, D.; Izumrudov, V. A. *Bioconjugate Chem.* **2007**, *18*, 922–928.